Available online at www.sciencedirect.com

ScienceDirect

Energy Procedia 38 (2013) 919 – 925

Energy Procedia

SiliconPV: March 25-27, 2013, Hamelin, Germany

Lift-off of free-standing layers in the kerfless porous silicon process

Sarah Kajari-Schröder[a,*], Jörg Käsewieter[a], Jan Hensen[a], Rolf Brendel[a,b]

[a]*Institute for Solar Energy Research Hamelin, D-31860 Emmerthal, Germany*
[b]*Institute of Solid-State Physics, Leibniz Universität Hannover, D-30167 Hannover, Germany*

Abstract

We discuss the lift-off of free-standing epitaxially grown silicon layers from the porous silicon (PSI) process, which is a kerfless wafering technology. The lift-off is a crucial step in the PSI cycle. A high-porosity layer serves as a mechanically weak layer for lift-off and consists of widely spaced silicon bridges with thicknesses of 40-100 nm. The low width leads to a 33-fold stress enhancement in the bridges, making them break when a force is applied while the epitaxial layer and the substrate remain intact. We perform the free-standing lift-off with a curved vacuum chuck. A vacuum pressure of 0.2 bar is sufficient for controlled peeling off of the 30-50 µm thick silicon layers. We simulate the stresses and the displacements of the epitaxial layer in the lift-off process close to the first non-broken bridge. We demonstrate the defect-free lift-off of 8 of 9 of 9 x 9 cm^2 layers from 6" substrates.

Keywords: Porous silicon; lift-off; layer transfer; kerfless wafering

1. Introduction

Despite the drastic reductions in the wafer price it still comprises about 40 % of today's module price. This is the reason for the wafer thickness and kerfloss reductions advocated in the international technology roadmap PV by 2020 [1]. The porous silicon (PSI) process [2,3] is one of several kerfless wafering techniques [4,5] promising to fulfill or even surpass these requirements. In this process a thick substrate is electrochemically porosified, forming a low porosity top layer and a high porosity buried layer. At high temperature of 1100°C the porous layer reorganizes and we epitaxially grow a silicon layer of thicknesses in the range of 30-50 µm. The reorganized buried high porosity layer is a mechanically weak breaking surface for the lift-off of the epitaxial layer, which serves as the absorber. The substrate re-enters the PSI cycle and repeatedly serves as the growth substrate [6].

doi:10.1016/j.egypro.2013.07.365

The lift-off process, which separates the epitaxial layer from the substrate, is a crucial step in the PSI process. The absorber layer needs to be defect-free after the lift-off. Defects can manifest in the form of cracks or torn-out pieces from the epitaxial layer. Additionally, no defects should be introduced into the substrate wafer that can limit the re-usability of the substrate wafer, e.g. chipping from the substrate wafer.

There are two general options for a lift-off process: encapsulating the epitaxial layer before lift-off, thus mechanically supporting the layer, or free-standing lift-off. While we find encapsulated lift-off to be reliable and robust, lifting off free-standing PSI layers opens up further options for solar cell processing and eliminates the risk of contaminating the substrate with encapsulant. So far we have achieved the highest solar cell efficiencies on PSI layers with free-standing layers [8]. Therefore in this contribution we discuss a mechanical lift-off concept for free-standing PSI layers.

2. Separation layer morphology

Fig. 1 shows a scanning electron micrograph (SEM) image of a reorganized porous layer before and Fig. 2 after lift-off. The separation layer connects the substrate and the epitaxial layer by bridges that are typically 40-100 nm wide in the narrowest point. The thickness of the separation layer is about 200 nm. The typical distance of the bridges varies with the etching parameters and is in the range of 200-1000 nm in the depicted case. Therefore the cumulative cross sectional area of the narrowest points of the bridges is only about 3 % of the total substrate area.

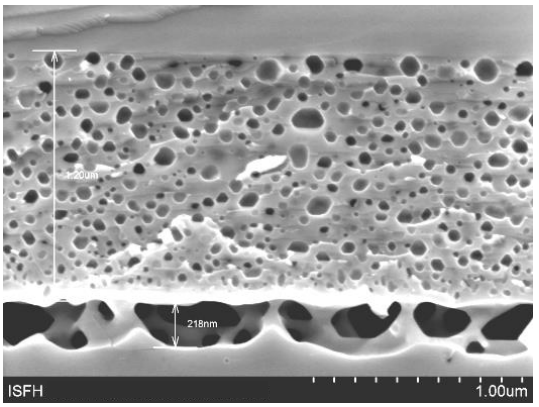

Fig. 1. SEM image of the porous silicon layer after epitaxial deposition. The substrate is at the bottom of the image, the epitaxial layer on top

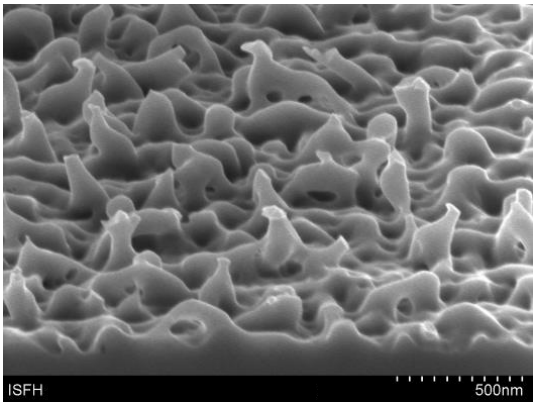

Fig. 2. Tilted SEM image of the separation layer on the substrate after lift-off.

3. Free-standing lift-off

3.1. Concept

For lift-off the bridges of the separation layer have to break, while the whole of the epitaxial layer and the substrate need to stay intact. A force F applied perpendicular to the surface of the substrate is focused in the thin bridges of the separation layer. With a relative cross sectional area A_{bridges} of the bridges of 3

% the stress $\sigma_{\text{bridges}} = F/A_{\text{bridges}}$ in the bridges is enhanced by a factor of about $A_{\text{epi}}/A_{\text{bridges}} = 100\ \%/3\ \% = 33$ with respect to the stress $\sigma_{\text{epi}} = F/A_{\text{epi}}$ in the epitaxial layer. A typical silicon wafer breaks at stresses in the order of 300 MPa [7]. On an area of 12.5 x 12.5 cm^2 this corresponds to a lift-off force of $F_{\text{lift-off}} = 47$ kN. We expect that the silicon bridges in the separation layer have an even higher breakage stress due to their thermally reorganized structure. The magnitude of the perpendicular lift-off forces for the full area is therefore too high even for the thin silicon bridges to make such a process feasible.

In order to reduce the forces necessary for lift-off we use a setup that breaks the bridges consecutively by peeling off the layer instead of forcing a simultaneous breakage of the bridges. Fig. 3 sketches our concept for the mechanical lift-off of free-standing PSI layers. We apply vacuum of about 0.2 bar through a chuck with a curvature radius of 0.75 m. The chuck surface is in contact with the PSI layer and is slowly rolled over the epitaxial layer. A related concept was presented in [9].

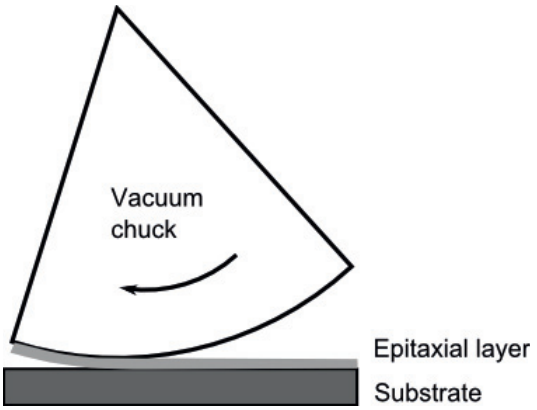

Fig. 3. Lift-off concept for free-standing PSI layers. A vacuum chuck is moved in a rolling motion across the epitaxial layer.

Fig. 4. Photographic image of the tool during lift-off. The direction of motion corresponds to the sketch in Fig. 3.

3.2. Numerical model

For an appropriate design of the lift-off tool it is necessary to mechanically understand free-standing lift-off process. In particular we are interested in how the required force for lift-off varies with the progress of the lift-off process. Insight into this offers the potential to optimize the pressure distribution in the chuck for efficient lift-off. As a first step towards this we therefore perform 3-dimensional mechanical finite element method (FEM) simulations with COMSOL Multiphysics of the setup sketched in Fig. 5. Here a 30 µm epitaxial silicon layer is on top of a 200 nm thick separation layer, which consists of equally spaced bridges of 100 nm width. The low-porosity starting layer is approximated as bulk silicon. The bridges have a rotational symmetry and are rounded so that no sharp points exist that would cause numerical divergences. On the left the separation layers is already released, i.e. free of bridges, on a lift-off distance of 0-30 µm. Underneath the separation layer is a silicon substrate of thickness 300 µm. We simulate one strip with a width of 1 µm of this setup, containing one line of bridges, and use periodic boundary conditions to account for extended samples. Due to the low curvature the individual bridges still

locally experience a force perpendicular to the substrate surface. Therefore we apply a uniform suction pressure of $\sigma = 1\ \mathrm{N/m^2}$ to the epitaxial layer, while the substrate is fixed.

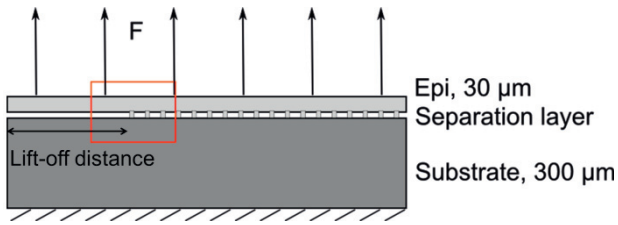

Fig. 5. Schematic view of the simulated setup. A uniform force is applied to the epi surface, the back of the substrate is fixed. The separation layer is already lift-off on the left of the sample. The red square denotes the zoom of Fig. 5.

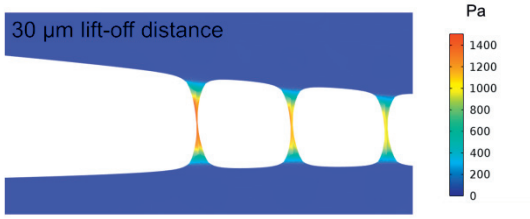

Fig. 6. Zoom into the deformation calculated from a FEM simulation of the situation sketched in Fig. 4. The deformation is scaled by a factor of $5 \cdot 10^8$ for better visibility.

3.3. Variation of lift-off distance

Figure 6 shows a slice plot of the simulated deformation of the separation layer, scaled up by a factor of $5 \cdot 10^8$ for better visibility. In this case the lift-off distance is 30 µm. The epitaxial layer in this part is displaced farther than the part that is still attached despite the uniformly applied force. The lift-off part of the epitaxial layer acts as a lever. As a result the stress concentration in the first remaining bridge is higher than in the other remaining bridges. This bridge will thus be broken next.

Figure 7 shows surface plots of the first principal stress with the lift-off distance 10 µm (top) and 30 µm (bottom) on the left of the images, respectively. The scaling is identical in both figures, thus directly showing the higher stress intensity in the first remaining bridge on the left of the images in comparison with the further bridges on the right. Also, the stress enhancement in the first remaining bridge is higher the longer the lift-off length is, as depicted in Fig. 8.

In the limit of zero lift-off length, i.e. if the separation layer has bridges on both ends of the sample, the stress intensity in the outermost bridges is not elevated in comparison to bridges in the center of the sample. As a consequence the initial lift-off point is particularly demanding with respect to the vacuum pressure applied. Layers that are in principle well cleavable with the presented setup may still suffer from difficulties in the initial lift-off point. On the other hand, already a small initial lift-off in one corner facilitates the continued release of the remaining layer.

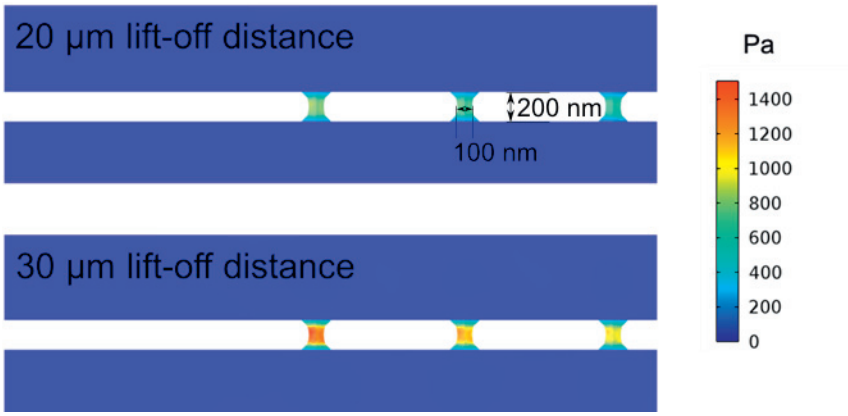

Fig. 7. Slice of the simulated separation layer with a lift-off distance of 20 µm (top) and 30 µm (bottom). The left-most bridge is the first bridge that is not yet broken. The color code depicts the magnitude of the first principal stress.

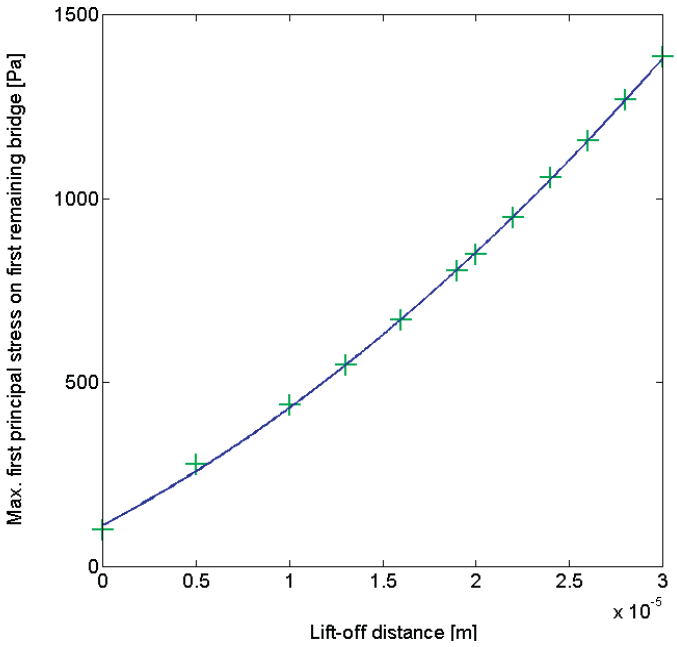

Fig. 8. Maximum of the first principal stress on the first remaining bridge in dependence on the lift-off length.

3.4. Experimental application

We apply the lift-off concept presented in this contribution to PSI layers. The layers are grown on 6" round substrates with a non-etched rim of about 1 cm. We define the area for lift-off by laser scribing a 9 x 9cm^2 square into the PSI layer. We mask the vacuum chuck with adhesive foil with a central cut out

area of 9.5 x 9.5cm^2, within this square the vacuum pressure is applied to the epitaxial layer. We align the laser scribed area such that the lift-off starts at a corner and proceeds diagonally with respect to the square, see Fig. 9. This reduces the required forces for the initial lift-off by limiting the width of simultaneous lift-off. However, this setup implies that the vacuum pressure may not be reduced as strongly with the lift-off distance as suggested by Fig. 8, as the length of the lift-off front grows in the first half of the process. We apply the lift-off process to 9 PSI layers that are etched with the same parameters. 8 of 9 layers detach without a visible defect such as cracks in the PSI layer. Fig. 10 shows a photograph of a PSI layer lifted-off with the described method. Due to the low thickness of 30 µm the layer is highly flexible.

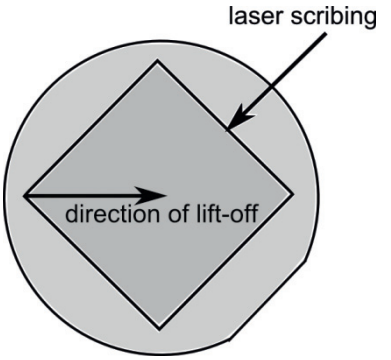

Fig. 9: Sketch of the sample orientation during lift-off.

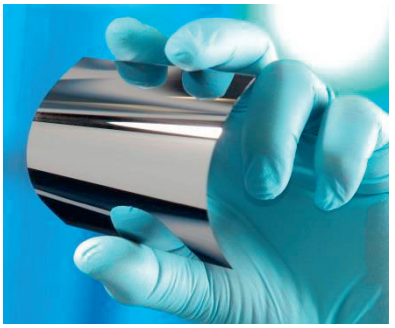

Fig. 10: Photograph of a 30 µm thick 9x9cm^2 large PSI layer.

4. Conclusions

The lift-off concept discussed in this contribution utilizes a scheme of subsequent breakage of the separation layer bridges. This reduces the forces required for lift-off drastically, as only a line of bridges at the fracture front breaks simultaneously. The longer the lift-off length is in the process, the more the stresses are focused specifically in the first remaining bridge. As a result, the actual challenge in operating this tool is to achieve initial lift-off, while requirements for continued lift-off are much lower. We have applied this lift-off concept on epitaxial layers which were laser scribed to 9x9 cm^2 on 6" substrates. We realize a crack-free lift-off yield of 8 of 9 layers.

In the industrialization of the PSI process, the lift-off process, freestanding or supported, is crucial. Without defect-free lift-off yield in the high 90 % range the cost reduction potential cannot be exploited. Even worse than a damaged PSI layer is a damaged substrate, as it is used repeatedly in the PSI cycle. However, with the lift-off concept discussed in this contribution we demonstrated the feasibility of free-standing lift-off. This now enables a range of solar cell processes that would not be possible in a lift-off scheme where the PSI layer is permanently attached to a carrier, e.g. further high temperature steps after lift-off.

Acknowledgements

The authors thank Renate Winter for sample preparation and Johannes Aprojanz for performing simulations. We gratefully acknowledge financial support by the Renewable Energy Corporation.

References

[1] International Technology Roadmap for Photovoltaic (ITRPV.net) Results 2011, March 2012 full edition. Retrieved 19.11.2012

[2] H. Tayanaka and T. Matsushita, Separation of thin epitaxial Si film on porous Si for solar cells, in Proceedings of the 6th Sony Research Forum, 1996, pp. 556

[3] R. Brendel, "A novel process for ultrathin monocrystalline silicon solar cells on glass", Proceedings of the 14th EUPVSEC, Barcelona, Spain, 1997, pp. 1354–1357,

[4] F. Dross, A. Milhe, J. Robbelein, I. Gordon, P.-O. Bouchard, G. Beaucarne, J. Poortmans, "Slim-Cut: A kerf-loss-free method for wafering 50-µm-thick crystalline Si wafers based on stress-induced lift-off", Proceedings of the 23rd EU PVSEC, Valencia, (WIP, Munich; 2008), p. 1278-1281

[5] F. Henley, A. Lamm, S. Kang, Z. Liu, L. Tian, "Direct Film Transfer (DFT) Technology for kerf-free silicon wafering", Proceedings of the 23rd EU PVSEC, Valencia, (WIP, Munich; 2008), p. 1090-1093

[6] V. Steckenreiter, J. Hensen, A. Knorr, E. Garralaga Rojas, S. Kajari-Schröder, and R. Brendel, „Reconditioning of silicon substrates for manifold re-use in the layer transfer process with porous silicon", PVSEC-22, Hangzhou, 2012

[7] J. H. Petermann, D. Zielke, J. Schmidt, F. Haase, E. G. Rojas, and R. Brendel, 19%-efficient and 43 µm-thick crystalline si solar cell from layer transfer using porous silicon, Progress in Photovoltaics 20, 1-5, (2011).

[8] R. Koepge, S. Schoenfelder, T. Giesen, C. Fischmann, A. Verl and J. Bagdahn, „The influence of transport operations on the wafer strength and breakage rate", Proceedings of the 26th EU PVSEC, Hamburg, Germany, 2011, pp. 2072-2077.

[9] K. Nakagawa et al., "Method of producing thin-film single-crystal device, solar cell module and method of producing the same", EP 1 069 602 A2